AAPS PharmSciTech (2020) 21:243
DOI: 10.1208/s12249-020-01783-0

Check for updates

Research Article

Theme: Pharmaceutical Thermal Processing - An Update
Guest Editors: Feng Zhang, Michael Repka and Suresh Bandari

Fabrication of Taste-Masked Donut-Shaped Tablets *Via* Fused Filament Fabrication 3D Printing Paired with Hot-Melt Extrusion Techniques

Honghe Wang,[1] Nagireddy Dumpa,[1] Suresh Bandari,[1] Thomas Durig,[2] and Michael A. Repka[1,3,4]

Received 30 March 2020; accepted 10 August 2020

Abstract. The objective of this work was to develop taste-masked donut-shaped tablet formulations utilizing fused filament fabrication three-dimensional printing paired with hot-melt extrusion techniques. Caffeine citrate was used as the model drug for its bitter taste, and a 3-point bend test was performed to assess the printability of filaments. The stiffness constant was calculated to represent the printability by fitting the breaking distances and stress data into Hooke's law. The formulations without Eudragit E PO (F6) and with Eudragit E PO (F7) filaments exhibited the desired hardness with a "k" value of 48.30 ± 3.52 and 45.47 ± 3.51 g/mm^3 ($n = 10$), respectively, and were successfully printed. The donut-shaped tablets were 3D printed with 10, 50, and 100% infill densities. *In vitro* dissolution studies were performed in simulated salivary fluid (pH 6.8, artificial saliva) to evaluate the taste-masking efficiency of the printed donuts. In the first minute, the concentrations of caffeine citrate observed in the dissolution media from all the printed donuts were less than the bitter threshold of caffeine citrate (0.25 mg/mL). Formulation F7, which contained Eudragit E PO copolymer, demonstrated better taste-masking efficiency than formulation F6. Furthermore, both formulations F6 and F7 demonstrated immediate drug release profiles in gastric medium (10% infill, >80% release within 1 h). Taste-masked caffeine citrate formulations were successfully developed with donut shapes, which will enhance appeal in pediatric populations and increase compliance and patient acceptance of the dosage form.

KEY WORDS: donut-shaped design; fused filament fabrication; hot-melt extrusion; Repka-Zhang test; taste masking; three-dimensional printing.

INTRODUCTION

Oral drug delivery is the most employed and convenient of all drug administration routes. A significant number of active pharmaceutical ingredients (APIs) used in oral drug delivery systems have a bitter taste (1). The bitterness of oral drug delivery systems influences compliance and patient acceptance of dosage forms (2), especially in pediatric populations. The mechanisms of commonly used taste-masking techniques can be summarized as three aspects: a physical barrier, chemical or solubility modification of active pharmaceutical ingredients, and the formation of solid dispersions (3). Various methods to mask the taste of bitter APIs are lipid barrier systems (4), cyclodextrin inclusion (5), film coatings (6), ion-exchange resins (3,7), microspheres (8), solid lipid pellets (9), and microencapsulation (10).

Hot-melt extrusion has been employed as a novel manufacturing technique of various solid oral dosage forms in the last two decades. It was used in the production of immediate-release dosage tablets (11,12), modified-release formulations including sustained release dosage forms (13–16), enteric release formulations (17), targeted release systems (18), chrono-modulated drug delivery systems (19), and novel taste-masked and abuse deterrence formulations (11). Taste masking is achieved by modifying drug release from the polymer matrix to prevent bitter APIs from contacting the patient's taste buds (20). HME is a continuous, solvent-free process, has a short processing time, and is easy to scale-up, and several polymer-carriers and other additives used during extrusion processing are generally known to be safe for consumption (21,22). HME for manufacturing taste-masking dosage forms is, therefore, a robust, cost-effective technique and has great potential for industrial scale-up.

[1] Department of Pharmaceutics and Drug Delivery, School of Pharmacy, The University of Mississippi, University, Mississippi 38677, USA.
[2] Ashland Specialty Ingredients, Wilmington, Delaware 19808, USA.
[3] Pii Center for Pharmaceutical Technology, The University of Mississippi, University, Mississippi 38677, USA.
[4] To whom correspondence should be addressed. (e–mail: marepka@olemiss.edu)

aaps
Published online: 27 August 2020

Three-dimensional (3D) printing is a layer-by-layer manufacturing technique that produces 3D real objects from computer-aided designs using plastic and metal materials (23,24). Fused filament fabrication (FFF) is a nozzle-based deposition system that creates solid objects by successive deposition of strands of molten polymers layer by layer *via* the nozzle of a moving printhead (25,26). FFF has several significant advantages such as low-cost manufacturing, a compatible downstream to take advantages of thermotolerant pharmaceutical polymers and APIs through hot-melt extrusion (HME), and the ability to design and manufacture novel drug delivery systems (27–29). Personalized medicine is a key factor for future improvement in disease treatment and is administered to individual patients (30). However, there is a lack of tailor-made taste-masking techniques for the masking of the unpalatable tastes of several drugs (31,32).

Compared with traditional pharmaceutical product manufacturing processes, the combination of HME and 3D-printing technology has two advantages: (1) the ability to fabricate immediate-release tablets, modified-release tablets, and other novel drug delivery systems and (2) the capability to produce more complex structured dosages and personalized drug products. Moreover, the combination of these two technologies reduces the downstream process that traditional manufacturing techniques involve, including milling extrudates, granulation, sieving, compressing, and coating, and thus renders them more efficient and economical (33,34). Furthermore, 3D printing is a novel technology in the pharmaceutical industry, providing an effective solution for individualized, complex, and customized production of oral drug delivery systems (35). 3D-printing technology combines digital design, manufacturing, and controls together, which is an accurate, timesaving, continuous process to meet individual patient needs (36). The combination of HME and 3D printing could be applied as a fabrication tool within digital health for the remote manufacture and dispensing of personalized formulations having doses, shapes, and sizes that are optimized for the patient. The therapy and medication adherence may be enhanced owing to the flexibility and autonomy of the treatment process provided by 3D printing (37). HME was employed to develop CC feedstock filaments using HPC and EPO as matrix polymers. Eudragit® E PO, a cationic copolymer based on dimethyl aminoethyl and neutral methacrylic esters, dissolves at pH < 5 and remains intact at neutral pH, which offers a potential application for taste masking (38).

Caffeine citrate, an odorless, bitter-tasting, Biopharmaceutics Classification System (BCS) class-I drug, was chosen as a model drug. It has a rapid dissolution rate in the oral cavity; thus, taste masking can be achieved by retarding the dissolution process using HME and 3D printing. The novelty of this investigation is to apply pair-FFF 3D printing with HME technology to design and fabricate tailor-made taste-masked donut-shaped tablets to enhance patient compliance, especially in pediatric populations.

MATERIALS AND METHODS

Materials

Caffeine citrate (CC) was purchased from Fisher Scientific (Pittsburgh, PA, USA). Klucel HPC, HF, and LF, and Benecel HPMC K4M were donated by Ashland Inc. (Covington, KY, USA). Eudragit E PO was supplied by Evonik Industries (Essen, Germany). All other reagents were of analytical grade.

Methods

Formulations

Initially, HPC LF, a commonly used polymer for 3D printing, was chosen to develop the formulations (Table I). HPMC K4M was used to achieve desirable mechanical properties and printability of filaments, and Eudragit E PO was added to improve the taste-masking ability of the 3D-printed donut-shaped tablets.

Hot-Melt Extrusion

The extruder (Thermo Fisher Scientific, Waltham, MA, USA) used in this study was a co-rotating, twin-screw extruder with 11 mm diameter screws, a length:diameter ratio of 40:1, and eight electrically heated zones. Physical mixtures of formulation ingredients were extruded at 155°C and a screw speed of 50 rpm. A standard screw configuration with three mixing zones provided by Thermo Fischer and a 1.5-mm round die was used to extrude filaments for 3D printing. The filaments were cooled and straightened using a conveyor belt at the extruding speed before loading into the 3D printer. Polylactic acid (PLA) without drug load was used as a reference to test the stiffness constant.

Differential Scanning Calorimetry

A differential scanning calorimtery (DSC) system (TA Instruments, New Castle, DE, USA) was used to study the crystallinity of the drug, the thermostability of the ingredients, and the nature of the drug in the filaments. Samples weighing 4–6 mg (pure ingredients and milled filaments) were sealed into aluminum pans and placed on the testing zone, then heated to the temperature range 25–250°C at a rate of 20°C/min. Nitrogen was used as the purge gas at a flow rate of 50 mL/min. The associated Pyris DSC software was used to analyze the data and the DSC thermograms.

Fused Filament Fabrication 3D Printing

Donut-shaped structures were designed online using Autodesk Tinkercad software (Tinkercad, Autodesk Inc., CA, USA) and saved as gcode files for printing. A

Table I. Compositions of the Formulations

Formulation	Drug (%, *w*/*w*)	Polymer (*w*/*w*)
F1	5	95% HPC LF
F2	10	90% HPC LF
F3	15	85% HPC LF
F4	20	60% HPC HF + 20% Eudragit EPO
F5	20	60% HPC LF + 20% HPMC K4M
F6	15	65% HPC LF + 20% HPMC K4M
F7	15	60% HPC LF + 20% HPMC K4M + 5% Eudragit EPO

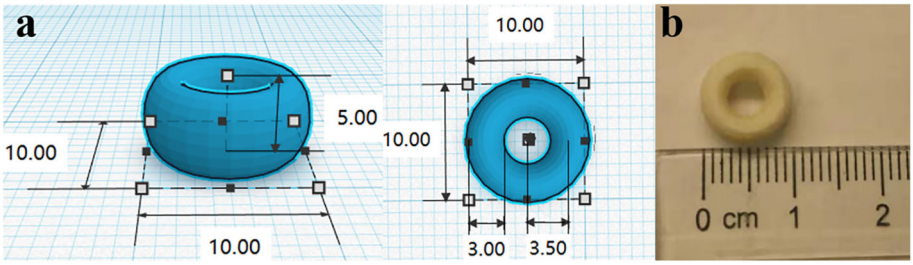

Fig. 1. Dimensions of 3D-printed tablets. **a** The view of tablet design (units: mm). **b** Conventional photograph of the 3D-printed tablet

commercial FFF 3D printer (Prusa i3 3D desktop printer, Prusa Research, Prague, Czech Republic) was used to print donut-shaped tablets, while printing operation software (CURA version 15.04; Ultimaker, Geldermalsen, Netherlands) was used to adjust the printing parameters. Donut dimensions were as follows (donut shape; diameter, 10 mm; height, 5 mm; radius (the distance between the tablet center to the tube center), 3.5 mm; tube thickness, 3 mm; wall thickness, 0.2 mm) (Fig. 1). The printing temperature was 200°C, while the bed temperature was 60°C, and the tablets were printed at three different (10, 50, and 100%) infill densities at a speed of 60 mm/s. The degradation temperature of CC is over 250°C, and all the excipients were stable at the processing temperature (21,33).

The Repka-Zhang Test

In this study, Repka-Zhang methods were adopted to perform 3-point bend tests to evaluate the printability of filaments (33). A TA-XT2 analyzer (Texture Technologies, Hamilton, MA, USA) and the TA-95N probe set were used for the flexibility and brittleness tests. The filament samples were cut into 6 cm rods, then placed on the sample holder (25 mm width gap). The blades moved at a speed of 10 mm/s until reaching 20 mm below the tested sample. Testing for each single filament formulation was repeated ten times. Polylactic acid was used as a reference material to compare the differences between commercially available filaments and extruded filaments.

Preparation of Tablets by Direct Compression

Conventional immediate-release tablets were formulated by direct compression for comparison of their drug release characteristics with 3D-printed tablets. Based on the highest weights and drug loads of the 3DP tablets (100% infill), 220 mg of physical mixtures of each formulation was compressed into tablets using an 8-mm die at 50 bar pressure. Formulation ingredients consisted of caffeine citrate (13.6%), croscarmellose sodium (8%), magnesium stearate (0.5%), and microcrystalline cellulose (77.9%). A VK200 Vankel Varian tablet hardness tester (Agilent Technologies, Santa Clara, CA, USA) was used to test the hardness of the direct compression tablets.

Fourier Transform Infrared Spectroscopy

An Agilent Cary 660 Fourier transform infrared spectroscopy (FTIR) spectrophotometer (Agilent Technologies, Santa Clara, CA, USA) was used to investigate interactions between the API and polymers over a 600–4000-cm^{-1} range. The FTIR spectra of the API, polymers, and milled extrudates were recorded.

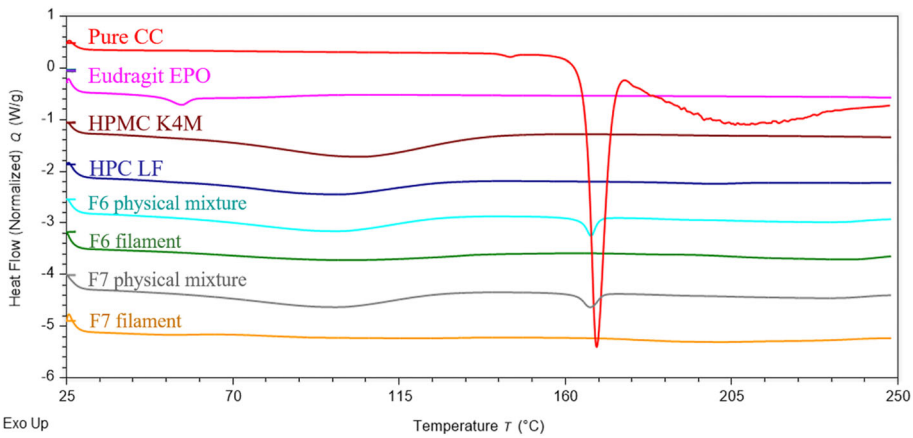

Fig. 2. DSC thermogram of caffeine citrate, HPC LF, HPMC K4M, Eudragit E PO, and formulations F6 and F7. F6: 15% CC, 20% HPMC K4M, and 65% HPC LF. F7: 15% CC, 20% HPMC K4M, 60% HPC LF, and 5% Eudragit EPO

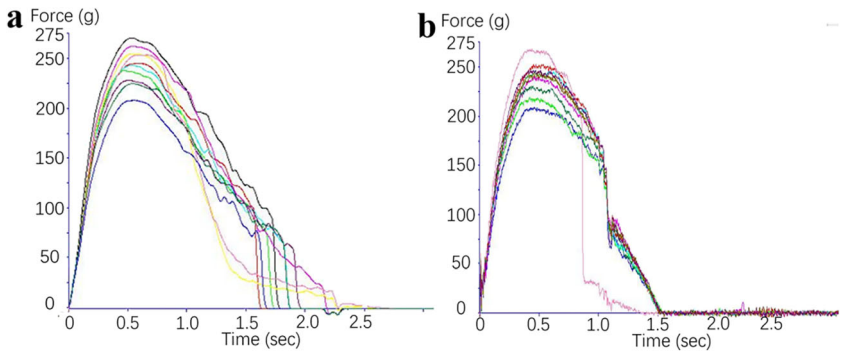

Fig. 3. The force-time curve of the 3-point bend test of filaments F6 and F7. **a** F6 filaments; **b** F7 filaments

Scanning Electron Microscope

A Hummer 6.2 sputtering system (Anatech LTD, Springfield, VA, USA) was used to investigate the surface morphology of the filaments and the cross-sections of 10, 50, and 100% infill printed tablets. The scanning electron microscope (SEM) apparatus (JEOL JSM-5600) operating system was set at an accelerating voltage of 5.0 kV for imaging (39). Magnifications of ×25, ×50, ×100, and ×200 were investigated to understand the morphology of printed tablets.

In Vitro Dissolution Studies

A United States Pharmacopeia (USP) dissolution apparatus I (Hanson SR8-plus; Hanson Research, Chatsworth, CA, USA) was employed to perform the *in vitro* dissolution studies. Each experiment was assessed in triplicate, and the temperature was set at 37 ± 0.5°C. Gastric drug release occurred in 900 mL of 0.1 N HCl, and the basket rotation speed was 100 rpm. Samples were collected at 5, 10, 15, 30, 60, 90, and 120 min time point, diluted, and analyzed using a UV-Vis spectrophotometer at 273 nm.

Evaluation of Taste Masking

To assess the taste-masking ability of the 3D-printed tablets, *in vitro* drug release studies was assessed using 500 mL of artificial salivary media adjusted to pH 6.8 (40). The drug release was analyzed at 10 s intervals for 10 min using Pion dissolution apparatus equipped with a dynamic UV-Vis detector system (Rainbow Dissolution Monitor, Pion Inc., Billerica, MA, USA) at 273 nm. The basket rotation speed was set to 100 rpm. The concentrations of caffeine citrate at the 60-s timepoint were compared with caffeine citrate threshold concentration (41). The bitterness threshold concentration of caffeine citrate was reported as 0.25 mg/mL (42). All observations were done in triplicate.

Drug Release Kinetics

The *in vitro* drug release data was fitted into Zero-order, first-order, Higuchi, Hixson-Crowell equation, and Ritger-Peppas equation, to assess the rate and mechanism of drug release (43,44).

Zero-order:

$$\frac{Q}{Q_\infty} = kt$$

First-order:

$$\ln\left(1-\frac{Q}{Q_\infty}\right) = -kt$$

Higuchi:

$$\frac{Q}{Q_\infty} = kt^{\frac{1}{2}}$$

Table II. The 3-Point Bend Test of Filaments (Mean ± SD, $n = 10$)

Filament	Force (g)	Stress (g/mm^2)	Distance (mm)	k (g/mm^3)	Printability
F1	250.49 ± 11.01	141.75 ± 6.23	4.67 ± 0.36	51.35 ± 2.73	Yes
F6	247.60 ± 16.94	140.11 ± 9.59	4.62 ± 0.21	48.30 ± 3.52	Yes
F7	243.12 ± 18.58	137.58 ± 10.52	4.95 ± 0.27	45.47 ± 3.51	Yes
PLA	1216.35 ± 21.02	505.70 ± 8.74	4.00 ± 0	151.14 ± 4.65	Yes

Parameters: force (g), stress (g/mm^2), distance (mm), "k" value (g/mm^3), *and result of filament printability*

Table III. Drug Content of Filaments and Tablets of Formulations F6 and F7 (Mean ± SD, $n = 3$)

Formulation	F6 (%)	F7 (%)
Filament	98.74 ± 0.28	101.63 ± 1.47
Tablet		
10%	97.99 ± 0.46	100.69 ± 1.39
50%	98.71 ± 0.43	98.60 ± 2.54
100%	97.99 ± 0.50	99.64 ± 2.78

Hixson-Crowell equation:

$$\left(1-\frac{Q}{Q_\infty}\right)^{\frac{1}{3}} = -kt$$

Ritger-Peppas equation:

$$\ln\frac{Q}{Q_\infty} = n\ln t + \ln k$$

where ks are the different constants in five models, respectively. Q is cumulative amount of drug release at time t. Q_∞ is the amount of the drug dose.

RESULTS AND DISCUSSION

Formulation

Initially, the formulations prepared using HPC alone showed decreased dissolution rates in gastric fluid and pH 6.8 phosphate buffer media because of the swelling properties of HPC and the conventional circular shape of the tablets. Based on the above observations, the donut shape was designed to increase the surface area to volume ratio compared with common circular 3DP tablet shapes (45). Though filament F1 could be printed well, its 5% drug load content was too low to develop a tablet form in use. With the same ingredients, higher drug load content filaments F2 and F3 were extruded. However, filaments F2 and F3 were too soft to be fed into the 3D printer. HPC HF and HPC EF were not selected because they had a higher viscosity than HPC LF, which confers a softer texture to the filaments. Then, HPMC K4M, a common excipient for sustained release systems, was used to increase the hardness of filaments and decrease the dissolution rate in pH 6.8 media. Thus, developing tablets at a drug load much greater than 5% came to a reality. Eudragit E PO is a pH-sensitive polymer that is easily dissolved at pH < 5 (46), which powerfully masks the taste of ingredients because the polymer is insoluble in saliva and water. Thus, the taste-masking polymer Eudragit E PO was used for taste-masking ability of the formulations. Increasing Eudragit E PO or the API caused the decrease of printabilities of filaments. F6 and F7 finally exhibited great printability rather than F4 or F5.

Differential Scanning Calorimetry

DSC is a solid-state characterization technique, used widely for detecting thermal transitions of polymeric materials by measuring the heat required to transit phases. The DSC thermogram of CC (Fig. 2) exhibited an endothermic melting peak at around 168°C. However, the peak was absent in the extrudates, indicating the transformation of CC from the crystalline to the amorphous state. CC dispersed into the polymers; thus, its odor and bitter taste could be masked.

The Repka-Zhang Test

Both softness and brittleness of the filaments affect their printability. Brittle filaments are easily crushed to fragments

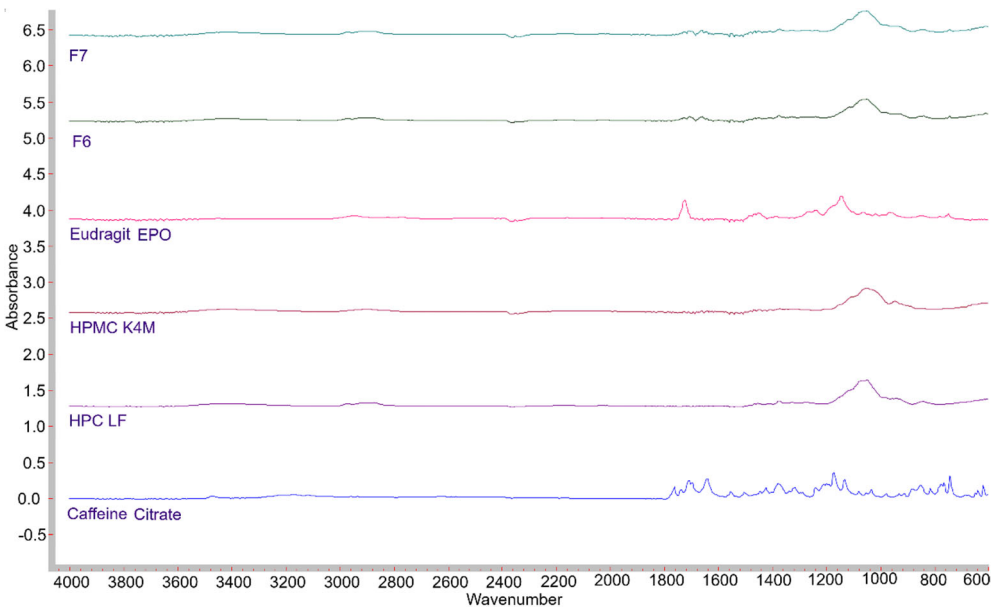

Fig. 4. FTIR spectra of extrudates; F6, F7, Eudragit E PO, HPMC K4M, HPC LF, and caffeine citrate

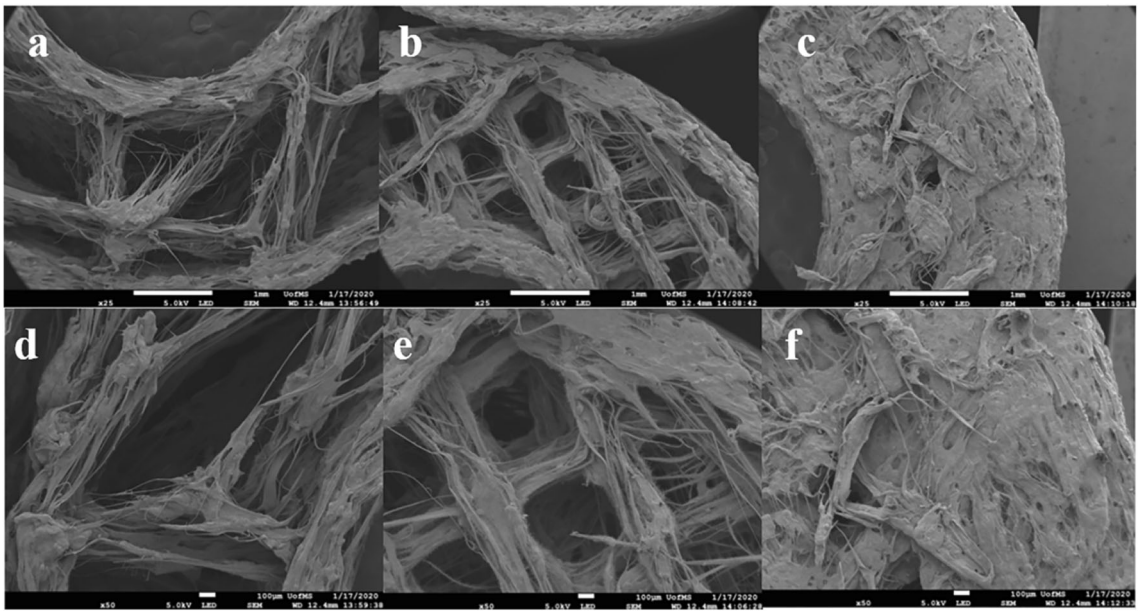

Fig. 5. SEM images of the F6 cross-section at × 25 and × 50 magnification levels: **a** 10% infill at × 25; **b** 50% infill at × 25; **c** 100% infill at × 25; **d** 10% infill at × 50; **e** 50% infill at × 50; **f** 100% infill at × 50

by gears inside the 3D printer and are difficult to feed into the 3D printer. Soft filaments are difficult to load into the 3D printer, have low abrasion resistance, usually cannot be conveyed by gears, and often block the head of the printer. The 3-point bend test is used to evaluate the breaking force, breaking distance, and breaking stress of a filament. The breaking stress is calculated from the breaking force divided by the cross-sectional area of the filament. In this study, the filaments were extruded *via* a 1.5-mm diameter die, but the PLA reference used for commercial 3DP has a 1.75-mm diameter. Thus, it is meaningful to compare breaking stresses rather than breaking forces. Greater breaking stress of a filament confers a harder filament texture. Likewise, a longer breaking distance results in a softer filament. According to the relationship curve of the polymer stress against the strain, higher breaking stresses or breaking distances indicate increased brittleness. In this study, the breaking distances of filaments were greater than PLA (4.00 ± 0 mm), while the stresses were less than PLA (505.70 ± 8.74 mm). Thus, brittleness was not considered (Fig. 3).

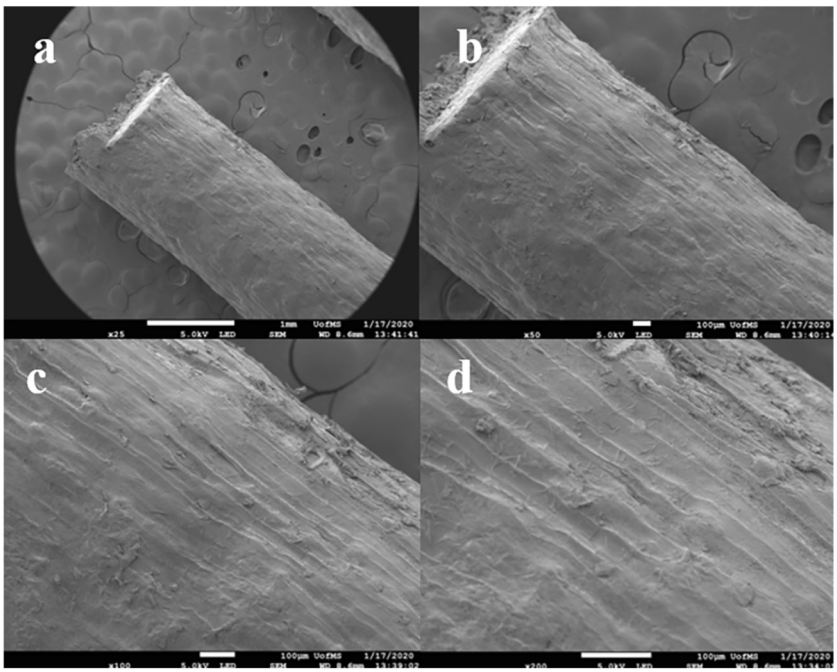

Fig. 6. SEM images of F6 filaments at **a** × 25, **b** × 50, **c** × 100, and **d** × 200 magnification levels

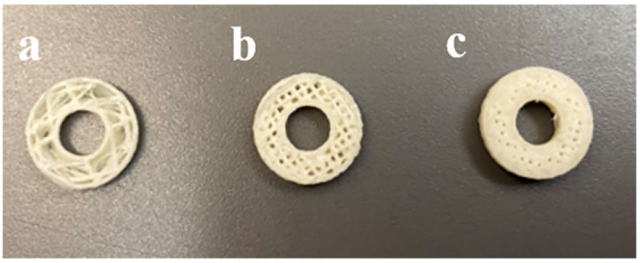

Fig. 7. The conventional photographs of the cross-sections of the F6 3D-printed tablets: **a** 10, **b** 50, and **c** 100% infill densities

Whether a filament is suitable for printing or not depends not only on the combination of the effects of stress and distance but other factors as well. Thus, Hooke's law is used to assess the printability of filament. A 3-point bend test figure consists of two parts, one is the elastic region, which is at the very beginning of a straight line, and the other is the plastic region, which is the remaining bending curve. Only in the elastic part (short bending distance) do the filaments exhibit elasticity, and when the force is removed, the filament will recover its shape. This phenomenon is similar to extending a spring. Thus, Hooke's law can be fitted. According to Hooke's law, $F = -kx$, "F" is the stress when the center of the filament is moved to distance "$-x$". To assure the data was on the straight elastic curve, a 2-mm bending distance was chosen, and corresponding stress was obtained from the figure. The stiffness constant "k" was calculated from the known data above. If the filament has a greater "k" value, printability will be improved. F1, F6, and F7 could be printed well due to their great "k" values. On the contrary, the "k" values of other filaments (F2, F3, F4, F5) were less than 40 g/mm^3, thus, they were not printable (Table II).

Direct Compression of Tablets

The physical mixture of the tablet blend had a good flowability and was compressed into 8 mm diameter circular-shaped tablets. The hardness of the directly compressed tablets was 9.82 ± 0.71 kp ($n = 10$), while the weight was 221.29 ± 4.50 mg ($n = 10$). The tablets were white with smooth surfaces without capping issues. Carr's index and Hausner ratio of physical mixtures were determined by measuring the poured bulk and tapped bulk volume after 100 taps in a graduated cylinder. Bulk density, 0.339 ± 0.01 g/mL ($n = 3$); tapped density, 0.412 ± 0.01 g/mL ($n = 3$); Carr's index (CI), 17.70 ± 0.17 ($n = 3$); and Hausner ratio (HR), 1.22 ± 0.003 ($n = 3$). CI was between 16 and 20, and HR was between 1.19 and 1.25, which was considered fair flowability (47).

Drug Content

The drug contents of filaments and 3D-printed tablets were 98–103% of the theoretical drug amounts, and there was no significant difference between the drug contents of filaments before and after 3D printing, indicating no drug degradation during 3D printing (Table III). The temperatures of the HME and 3D-printing process were 155 and 200°C, respectively. However, the degradation temperature of caffeine citrate is above 250°C, indicating that the API had good thermal stability during extrusion and 3D printing.

Fourier Transform Infrared Spectroscopy

FTIR was performed to determine the post-extrusion physical characterization of the extrudates (Fig. 4). Eudragit E PO spectra showed a significant absorbance peak at 1723 cm^{-1}, which represented C=O functional groups. This peak shifted to 1703 cm^{-1} in the spectra of the F7 formulation, indicating that the carbonyl group (proton-accepting group) in Eudragit E PO had a strong interaction with the hydroxyl group (proton-donating group) in HPC LF and HPMC K4M, inducing intermolecular hydrogen bond interactions.

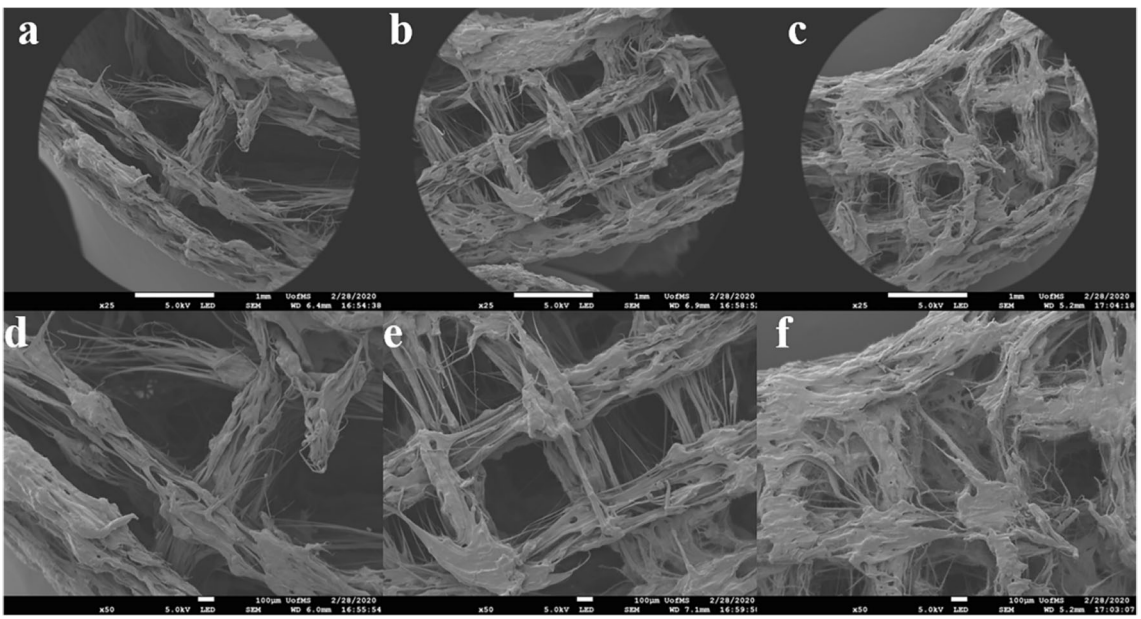

Fig. 8. SEM images of the F7 cross-section at × 25 and × 50 magnification levels: **a** 10% infill at × 25; **b** 50% infill at × 25; **c** 100% infill at × 25; **d** 10% infill at × 50; **e** 50% infill at × 50; and **f** 100% infill at × 50

Table IV. Weights of 3D-Printed Tablets F6 and F7 (Mean ± SD, n = 6)

Tablet infill	F6 (mg)	F7 (mg)
10%	101.3 ± 2.7	102.1 ± 4.8
50%	144.5 ± 5.7	147.2 ± 7.12
100%	225.1 ± 7.0	232.1 ± 5.42

From the caffeine citrate spectra, the peak at 3471 cm^{-1} corresponds to the enol O–H stretching vibrations, due to the energy increasing by HME. The peak at 1641 cm^{-1} corresponds to the amide structure (CO-NRR'). The caffeine citrate spectra showed a peak at 3168 cm^{-1}, representing the quaternary ammonium structure composed from the tertiary amine group in caffeine and the carboxyl group of citric acid. After the HME process, the crystal structure transformed into an amorphous form, and the two components caffeine and citric acid completely dispersed into the polymer matrix. Furthermore, the absence of the peak at 3168 cm^{-1} indicated the free tertiary amine group (proton-accepting group) did not form hydrogen bonding with the hydroxyl group (proton-donating group) in polymers; otherwise, it would shift to a lower wavenumber; thus, the bitter taste of caffeine may be masked due to physical entrapment of the API in the carrier (42).

Scanning Electron Microscope

SEM images of F6-printed tablets showed a significant difference between 10, 50, and 100% infill densities (Fig. 5). The surface was smooth, and the tablets showed a stepped construction, which accorded with the printing process layer on layer. The texture of 10% infill was the most diffuse and poorly compacted, and the 100% infill was the most compact. According to the *in vitro* dissolution test data, the increased compactness resulted in a decreased dissolution rate. The tablets with a weakly compact structure readily dissolved in solution, while it took relatively more time for their counterparts with compact structures. Furthermore, a compact structure caused a harder texture of the tablets. SEM images of F6 filaments exhibited a uniform width and smooth filament surfaces as a result of the stable HME process. There was no agglomeration on the surface, suggesting a completely miscible solid dispersion system (Fig. 6). The conventional photographs of the cross-section of tablets are shown in Fig. 7. SEM images of F7-printed tablets showed similar structures to the counterparts of F6 (Fig. 8), a greater infill percentage leading to a more compacted structure.

In Vitro Drug Release Study

The weights of 3D-printed tablets are provided in Table IV. HPC LF and HPMC K4M are widely used polymers known for eroding matrix in 3D printing, so they have properties conducive to modified-release drug delivery systems. Further, the decreased drug release rate in pH 6.8 media may moderately aid in taste masking. Conversely, 3D-printed tablets have a much more solid structure, decreasing the drug release rate. To attain desired drug release characteristics in 0.1 N HCl, donut-shaped 3D-printed tablets with a large surface area to volume ratio compared with conventionally shaped 3DP tablets were printed, which significantly increased the drug release rate. Furthermore, the wall of the pore at the center of the tablet is not easily accessible to saliva.

Dissolution profiles of FFF 3D-printed tablets with 10, 50, and 100% infill densities in 0.1 N HCl media are listed in Fig. 9. As expected, for both F6 and F7 tablets, tablets with 10% infill exhibited higher dissolution rates than the 50 and 100% infill tablets and exhibited more than 80% drug release in 60 min. This increased dissolution rate with 10% infill density compared with 50 and 100% infill may be attributed to the increased surface area because of the pores in the tablets. The release mechanism of CC can be explained by the fact that when the hydrophilic polymers contact an aqueous solution, they may swell and become an eroding matrix, and the hydrophilic drug CC releases from the eroding matrix (48).

Evaluation of Taste Masking

As shown in Fig. 10, the 3D-printed tablets with 10% infill exhibited higher dissolution rates than 50 and 100% infill densities. The tablets exhibited approximately 5% drug release in 60 s and less than 10% in 120 s. However, the concentrations of 100% infill tablets reached their maximum, because the amount of CC and the weight of the tablets were the greatest. The dissolution rate of F7 was less than that of the counterpart of F6 at the same drug infill percentage. The reason for this is that Eudragit E PO is a pH-sensitive

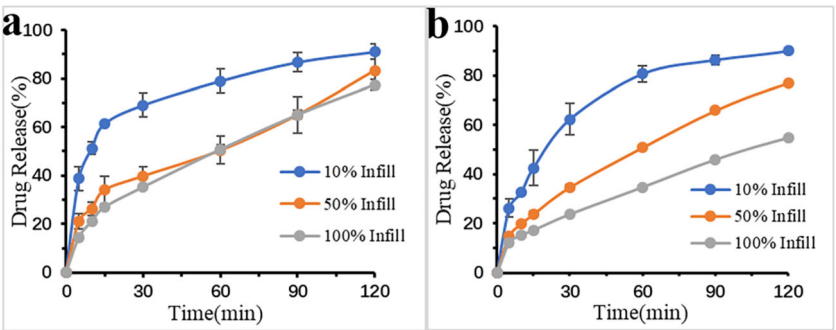

Fig. 9. The dissolution profiles of 3D-printed tablets in 0.1 N HCl media: **a** F6 and **b** F7

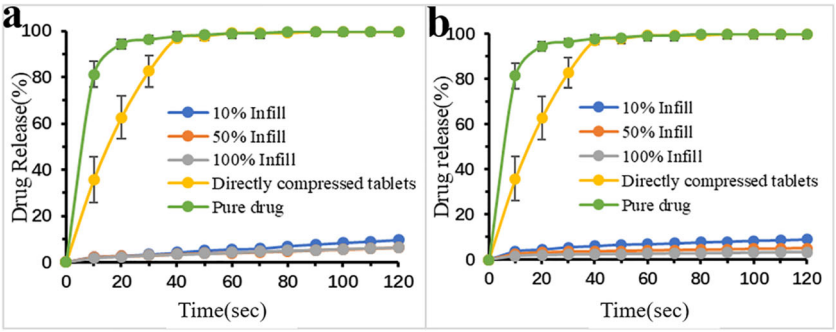

Fig. 10. The dissolution profiles of 3D-printed tablets in pH 6.8 artificial saliva media **a** F6, directly compressed tablets, and pure drug; **b** F7, directly compressed tablets, and pure drug

polymer and insoluble in the mouth but readily soluble in the stomach due to its polyacrylate molecular structure. Eudragit E PO, owing to its adhesive properties was not suitable for 3D printing above 5% in this study. Hence, Eudragit E PO, at 5%, exhibited improved taste-masking ability. Even the concentrations of 100% infill 3DP tablets in the first minute were less than the tasting threshold of caffeine citrate of 0.25 mg/mL (F6, 100% infill, 0.019 ± 0.001 mg/mL, $n = 3$; F7, 100% infill, 0.012 ± 0.001 mg/mL, $n = 3$) (42),. Therefore, the 3D-printed tablets could mask the bitter taste. Compressed tablets and pure drugs were evaluated for their drug release rates. The directly compressed tablets exhibited a 100% release in 50 s at pH 6.8. Similarly, the pure drug exhibited a 100% dissolution rate in 30 s. The 3D-printed donut-shaped tablets released more slowly than compressed tablets and pure drugs.

Drug Release Kinetics

The drug release was fitted into the mathematical models, and the correlation coefficients were calculated (Table V). Zero order was not fitted for 10% infill density tablets, but drug release of tablets with higher infill densities showed a relatively better correlation to zero-order kinetics. The Higuchi model best fit the drug release profiles, and a greater infill density showed a higher correlation coefficient. As for the Ritger-Peppas model, the slope $n < 0.45$, the drug release mechanism is Fickian diffusion; $0.45 < n < 1.00$ is characterized as anomalous (non-Fickian) transport; and for $n = 1.0$, zero-order release is predicted (49). The donut shape is considered mean properties between the cylinder and the sphere shape, and drug release was observed to be predominantly the diffusion mechanism.

Table V. *In Vitro* Release Kinetics of 3D-Printed Tablets F6 and F7

Infill	Correlation coefficient (R^2)					
	Zero-order	First-order	Higuchi	Hixson-Crowell	Ritger-Peppas	*n*
F6						
0.1 N HCl						
10%	0.686	0.940	0.890	0.872	0.962	0.268
50%	0.912	0.943	0.977	0.952	0.976	0.405
100%	0.946	0.989	0.997	0.984	0.997	0.515
pH 6.8 artificial saliva						
10%	0.983	0.985	0.963	0.984	0.968	0.617
50%	0.922	0.928	0.991	0.926	0.978	0.439
100%	0.943	0.948	0.995	0.946	0.991	0.500
F7						
0.1 N HCl						
10%	0.758	0.966	0.940	0.952	0.969	0.392
50%	0.945	0.968	0.998	0.994	0.998	0.532
100%	0.958	0.993	0.992	0.988	0.986	0.499
pH 6.8 artificial saliva						
10%	0.838	0.849	0.963	0.894	0.994	0.368
50%	0.737	0.744	0.991	0.741	0.987	0.261
100%	0.736	0.741	0.995	0.740	0.987	0.260

CONCLUSIONS

In this study, we successfully developed taste-masked tablets *via* fused filament fabrication 3D printing paired with hot-melt extrusion techniques. Three-point bend tests were performed, and the results were fitted into Hooke's law, which could explain the relationship between the data and the hardness of the filaments. The concentrations of caffeine citrate released from the 3DP donut-shaped tablets were less than the tasting threshold of caffeine citrate after 1 min, and the tablets exhibited desired drug release rates in 0.1 N HCl, indicating a taste-masking ability. The donut shape successfully modified the dissolution rates through HPC LF and HPMC K4M, leading to low dissolution rates. This study demonstrates that hot-melt extrusion has excellent potential for taste masking, and FFF 3D printing is a new approach for manufacturing potential drug delivery systems for patient-centric pediatric populations.

FUNDING INFORMATION

This project was also partially supported by Grant Number P30GM122733-01A1, funded by the National Institute of General Medical Sciences (NIGMS), a component of the National Institutes of Health (NIH) as one of its Centers of Biomedical Research Excellence (COBRE).

COMPLIANCE WITH ETHICAL STANDARDS

Conflict of Interest The authors declare that they have no conflict of interest.

REFERENCES

1. Maniruzzaman M, Boateng JS, Chowdhry BZ, Snowden MJ, Douroumis D. A review on the taste masking of bitter APIs: hot-melt extrusion (HME) evaluation. Drug Dev Ind Pharm. 2014;40(2):145–56. https://doi.org/10.3109/03639045.2013.804833.
2. Zheng JY, Keeney MP. Taste masking analysis in pharmaceutical formulation development using an electronic tongue. Int J Pharm. 2006;310(1–2):118–24. https://doi.org/10.1016/j.ijpharm.2005.11.046.
3. Tan DCT, Ong JJ, Gokhale R, Heng PWS. Hot melt extrusion of ion-exchange resin for taste masking. Int J Pharm. 2018;547(1–2):385–94. https://doi.org/10.1016/j.ijpharm.2018.05.068.
4. Petrovick GF, Breitkreutz J, Pein-Hackelbusch M. Taste-masking properties of solid lipid based micropellets obtained by cold extrusion-spheronization. Int J Pharm. 2016;506(1–2):361–70. https://doi.org/10.1016/j.ijpharm.2016.04.058.
5. Rachmawati H, Marbun EJ, Pamudji JS. Development of fast disintegrating tablet formula of ketoprofen-β-cyclodextrin inclusion complexes. Indian J Pharm. 2011;22(3):229–37. https://doi.org/10.14499/indonesianjpharm0iss0pp229-237.
6. Joshi S, Petereit HU. Film coatings for taste masking and moisture protection. Int J Pharm. 2013;457(2):395–406. https://doi.org/10.1016/j.ijpharm.2013.10.021.
7. Keating AV, Soto J, Tuleu C, Forbes C, Zhao M, Craig DQM. Solid state characterisation and taste masking efficiency evaluation of polymer based extrudates of isoniazid for paediatric administration. Int J Pharm. 2018;536(2):536–46. https://doi.org/10.1016/j.ijpharm.2017.07.008.
8. Gao Y, Cui FD, Guan Y, Yang L, Wang YS, Zhang LN. Preparation of roxithromycin-polymeric microspheres by the emulsion solvent diffusion method for taste masking. Int J Pharm. 2006;318(1–2):62–9. https://doi.org/10.1016/j.ijpharm.2006.03.018.
9. Petrovick GF, Kleinebudde P, Breitkreutz J. Orodispersible tablets containing taste-masked solid lipid pellets with metformin hydrochloride: influence of process parameters on tablet properties. Eur J Pharm Biopharm. 2018;122:137–45. https://doi.org/10.1016/j.ejpb.2017.10.018.
10. Khor CM, Ng WK, Kanaujia P, Chan KP, Dong Y. Hot-melt extrusion microencapsulation of quercetin for taste-masking. J Microencapsul. 2017;34(1):29–37. https://doi.org/10.1080/02652048.2017.1280095.
11. Nukala PK, Palekar S, Patki M, Patel K. Abuse deterrent immediate release egg-shaped tablet (Egglets) using 3D printing technology: quality by design to optimize drug release and extraction. AAPS PharmSciTech. 2019;20(2):80. https://doi.org/10.1208/s12249-019-1298-y.
12. Sadia M, Arafat B, Ahmed W, Forbes RT, Alhnan MA. Channelled tablets: an innovative approach to accelerating drug release from 3D printed tablets. J Control Release. 2018;269:355–63. https://doi.org/10.1016/j.jconrel.2017.11.022.
13. Maniruzzaman M, Boateng JS, Bonnefille M, Aranyos A, Mitchell JC, Douroumis D. Taste masking of paracetamol by hot-melt extrusion: an in vitro and in vivo evaluation. Eur J Pharm Biopharm. 2012;80(2):433–42. https://doi.org/10.1016/j.ejpb.2011.10.019.
14. Maniruzzaman M, Boateng JS, Snowden MJ, Douroumis D. A review of hot-melt extrusion: process technology to pharmaceutical products. ISRN Pharm. 2012;2012:436763–9. https://doi.org/10.5402/2012/436763.
15. Crowley MM, Zhang F, Repka MA, Thumma S, Upadhye SB, Battu SK, *et al.* Pharmaceutical applications of hot-melt extrusion: part I. Drug Dev Ind Pharm. 2007;33(9):909–26. https://doi.org/10.1080/03639040701498759.
16. Reddy Dumpa N, Bandari S, Repka AR. Novel gastroretentive floating pulsatile drug delivery system produced via hot-melt extrusion and fused deposition modeling 3D printing. Pharmaceutics. 2020;12(1). https://doi.org/10.3390/pharmaceutics12010052.
17. Nober C, Manini G, Carlier E, Raquez JM, Benali S, Dubois P, *et al.* Feasibility study into the potential use of fused-deposition modeling to manufacture 3D-printed enteric capsules in compounding pharmacies. Int J Pharm. 2019;569:118581. https://doi.org/10.1016/j.ijpharm.2019.118581.
18. Patil H, Tiwari RV, Repka MA. Hot-melt extrusion: from theory to application in pharmaceutical formulation. AAPS PharmSciTech. 2016;17(1):20–42. https://doi.org/10.1208/s12249-015-0360-7.
19. Dumpa NR, Sarabu S, Bandari S, Zhang F, Repka MA. Chronotherapeutic drug delivery of ketoprofen and ibuprofen for improved treatment of early morning stiffness in arthritis using hot-melt extrusion technology. AAPS PharmSciTech. 2018;19(6):2700–9. https://doi.org/10.1208/s12249-018-1095-z.
20. Juluri A, Popescu C, Zhou L, Murthy RN, Gowda VK, Chetan Kumar P, *et al.* Taste masking of griseofulvin and caffeine anhydrous using Kleptose Linecaps DE17 by hot melt extrusion. AAPS PharmSciTech. 2016;17(1):99–105. https://doi.org/10.1208/s12249-015-0374-1.
21. Tiwari RV, Polk AN, Patil H, Ye X, Pimparade MB, Repka MA. Rat palatability study for taste assessment of caffeine citrate formulation prepared via hot-melt extrusion technology. AAPS PharmSciTech. 2017;18(2):341–8. https://doi.org/10.1208/s12249-015-0447-1.
22. Lang B, McGinity JW, Williams RO 3rd. Hot-melt extrusion–basic principles and pharmaceutical applications. Drug Dev Ind Pharm. 2014;40(9):1133–55. https://doi.org/10.3109/03639045.2013.838577.
23. Arafat B, Qinna N, Cieszynska M, Forbes RT, Alhnan MA. Tailored on demand anti-coagulant dosing: an in vitro and in vivo evaluation of 3D printed purpose-designed oral dosage

forms. Eur J Pharm Biopharm. 2018;128:282–9. https://doi.org/10.1016/j.ejpb.2018.04.010.
24. Acosta-Velez FG. 3D pharming: direct printing of personalized pharmaceutical tablets. Polymer Science. 2016;2(1). https://doi.org/10.4172/2471-9935.100011.
25. Gioumouxouzis CI, Baklavaridis A, Katsamenis OL, Markopoulou CK, Bouropoulos N, Tzetzis D, *et al.* A 3D printed bilayer oral solid dosage form combining metformin for prolonged and glimepiride for immediate drug delivery. Eur J Pharm Sci. 2018;120:40–52. https://doi.org/10.1016/j.ejps.2018.04.020.
26. Melocchi A, Parietti F, Loreti G, Maroni A, Gazzaniga A, Zema L. 3D printing by fused deposition modeling (FDM) of a swellable/erodible capsular device for oral pulsatile release of drugs. J Drug Deliv Sci Technol. 2015;30:360–7. https://doi.org/10.1016/j.jddst.2015.07.016.
27. Chai X, Chai H, Wang X, Yang J, Li J, Zhao Y, *et al.* Fused deposition modeling (FDM) 3D printed tablets for Intragastric floating delivery of Domperidone. Sci Rep. 2017;7(1):2829. https://doi.org/10.1038/s41598-017-03097-x.
28. Goyanes A, Chang H, Sedough D, Hatton GB, Wang J, Buanz A, *et al.* Fabrication of controlled-release budesonide tablets via desktop (FDM) 3D printing. Int J Pharm. 2015;496(2):414–20. https://doi.org/10.1016/j.ijpharm.2015.10.039.
29. Skowyra J, Pietrzak K, Alhnan MA. Fabrication of extended-release patient-tailored prednisolone tablets via fused deposition modelling (FDM) 3D printing. Eur J Pharm Sci. 2015;68:11–7. https://doi.org/10.1016/j.ejps.2014.11.009.
30. Li Q, Wen H, Jia D, Guan X, Pan H, Yang Y, *et al.* Preparation and investigation of controlled-release glipizide novel oral device with three-dimensional printing. Int J Pharm. 2017;525(1):5–11. https://doi.org/10.1016/j.ijpharm.2017.03.066.
31. Zheng X, Wu F, Hong Y, Shen L, Lin X, Feng Y. Developments in taste-masking techniques for traditional Chinese medicines. Pharmaceutics. 2018;10(3). https://doi.org/10.3390/pharmaceutics10030157.
32. Arafat B, Wojsz M, Isreb A, Forbes RT, Isreb M, Ahmed W, *et al.* Tablet fragmentation without a disintegrant: A novel design approach for accelerating disintegration and drug release from 3D printed cellulosic tablets. Eur J Pharm Sci. 2018;118:191–9. https://doi.org/10.1016/j.ejps.2018.03.019.
33. Zhang J, Xu P, Vo AQ, Bandari S, Yang F, Durig T, *et al.* Development and evaluation of pharmaceutical 3D printability for hot melt extruded cellulose-based filaments. J Drug Deliv Sci Technol. 2019;52:292–302. https://doi.org/10.1016/j.jddst.2019.04.043.
34. Zhang J, Feng X, Patil H, Tiwari RV, Repka MA. Coupling 3D printing with hot-melt extrusion to produce controlled-release tablets. Int J Pharm. 2017;519(1–2):186–97. https://doi.org/10.1016/j.ijpharm.2016.12.049.
35. Zhang J, Yang W, Vo AQ, Feng X, Ye X, Kim DW, *et al.* Hydroxypropyl methylcellulose-based controlled release dosage by melt extrusion and 3D printing: structure and drug release correlation. Carbohydr Polym. 2017;177:49–57. https://doi.org/10.1016/j.carbpol.2017.08.058.
36. Goole J, Amighi K. 3D printing in pharmaceutics: A new tool for designing customized drug delivery systems. Int J Pharm. 2016;499(1–2):376–94. https://doi.org/10.1016/j.ijpharm.2015.12.071.
37. Awad A, Trenfield SJ, Gaisford S, Basit AW. 3D printed medicines: a new branch of digital healthcare. Int J Pharm. 2018;548(1):586–96. https://doi.org/10.1016/j.ijpharm.2018.07.024.
38. Xu J, Bovet LL, Zhao K. Taste masking microspheres for orally disintegrating tablets. Int J Pharm. 2008;359(1–2):63–9. https://doi.org/10.1016/j.ijpharm.2008.03.019.
39. Alshehri SM, Park JB, Alsulays BB, Tiwari RV, Almutairy B, Alshetaili AS, *et al.* Mefenamic acid taste-masked oral disintegrating tablets with enhanced solubility via molecular interaction produced by hot melt extrusion technology. J Drug Deliv Sci Technol. 2015;27:18–27. https://doi.org/10.1016/j.jddst.2015.03.003.
40. Marques MRC, Loebenberg R, Almukainzi M. Simulated biological fluids with possible application in dissolution testing. Dissolution Technologies. 2011;18(3):15–28. https://doi.org/10.14227/DT180311P15.
41. Bandari S, Dronam VR, Eedara BB. Development and preliminary characterization of levofloxacin pharmaceutical cocrystals for dissolution rate enhancement. J Pharm Investig. 2017;47(6):583–91. https://doi.org/10.1007/s40005-016-0302-8.
42. Pimparade MB, Morott JT, Park JB, Kulkarni VI, Majumdar S, Murthy SN, *et al.* Development of taste masked caffeine citrate formulations utilizing hot melt extrusion technology and in vitro-in vivo evaluations. Int J Pharm. 2015;487(1–2):167–76. https://doi.org/10.1016/j.ijpharm.2015.04.030.
43. Jeganathan B, Prakya V. Interpolyelectrolyte complexes of Eudragit® EPO with hypromellose acetate succinate and Eudragit® EPO with hypromellose phthalate as potential carriers for oral controlled drug delivery. AAPS PharmSciTech. 2015;16(4):878–88. https://doi.org/10.1208/s12249-014-0252-2.
44. Baishya H. Application of mathematical models in drug release kinetics of carbidopa and levodopa ER tablets. J Develop Drugs. 2017;06(02). https://doi.org/10.4172/2329-6631.1000171.
45. Goyanes A, Robles Martinez P, Buanz A, Basit AW, Gaisford S. Effect of geometry on drug release from 3D printed tablets. Int J Pharm. 2015;494(2):657–63. https://doi.org/10.1016/j.ijpharm.2015.04.069.
46. Abdelhakim HE, Coupe A, Tuleu C, Edirisinghe M, Craig DQM. Electrospinning optimization of Eudragit E PO with and without chlorpheniramine maleate using a design of experiment approach. Mol Pharm. 2019;16(6):2557–68. https://doi.org/10.1021/acs.molpharmaceut.9b00159.
47. Shah RB, Tawakkul MA, Khan MA. Comparative evaluation of flow for pharmaceutical powders and granules. AAPS PharmSciTech. 2008;9(1):250–8. https://doi.org/10.1208/s12249-008-9046-8.
48. Nokhodchi A, Raja S, Patel P, Asare-Addo K. The role of oral controlled release matrix tablets in drug delivery systems. Bioimpacts. 2012;2(4):175–87. https://doi.org/10.5681/bi.2012.027.
49. Ritger PL, Peppas NA. A simple equation for description of solute release I. Fickian and non-fickian release from non-swellable devices in the form of slabs, spheres, cylinders or discs. J Control Release. 1987;5(1):23–36. https://doi.org/10.1016/0168-3659(87)90034-4.